International Journal of Architectural, Civil and Construction Sciences
ISSN: 2415-1734
Vol:7, No:5, 2013

# The Impact of an Air-Supply Guide Vane on the Indoor Air Distribution

C.-C. Tsao, S.-W. Nien, W.-H. Chen, and Y.-C. Shih

***Abstract*—**Indoor air distribution has great impact on people's thermal sensation. Therefore, how to remove the indoor excess heat becomes an important issue to create a thermally comfortable indoor environment. To expel the extra indoor heat effectively, this paper used a dynamic CFD approach to study the effect of an air-supply guide vane swinging periodically on the indoor air distribution within a model room. The numerical results revealed that the indoor heat transfer performance caused by the swing guide vane had close relation with the number of vortices developing under the inlet cold jet. At larger swing amplitude, two smaller vortices continued to shed outward under the cold jet and remove the indoor heat load more effectively. As a result, it can be found that the average Nusselt number on the floor increased with the increase of the swing amplitude of the guide vane.

***Keywords*—**Computational Fluid Dynamics (CFD), dynamic mesh, heat transfer, indoor air distribution, thermal comfort.

## I. Introduction

IN modern society, most people spend a great part of their lifetime staying indoors. As a result, creating comfortably indoor environment plays an important role on people's indoor activities. Among those factors to create comfortably indoor environment, making comfortably thermal environment is one of the most important factors to satisfy human's sensation of "comfort". Thermal comfort is defined as "that condition of mind which expresses satisfaction with thermal environment" [1,2]. It is evaluated by two personal factors comprising activity level and thermal insulation of clothing as well as four environmental parameters, including air temperature, mean radiant temperature, air velocity, and air humidity. This study is motivated by creating the indoor environment with thermal comfort for humans.

Thermal comfort has close relation to the indoor air movement. However, air movement within a room depends upon several factors. For example, indoor air movement is often induced by the forced convective airflow supplied by an air-conditioning system. Also, temperature difference between the wall of a room and indoor air may cause indoor air movement, such as natural convection. Air movement caused by a differential pressure across the indoor structure may be considerable. The existence of doorways and apertures inside a room could have great impact on the indoor air movement. The opening and closing of doors coupling with people's movement may have important influence on the indoor air distribution. Moreover, the arrangement of furniture also has some effect on the indoor air movement.

Owing to the urgent demand of comfortable living indoors, many numerical studies [3-20] related to the prediction of indoor air distribution within a ventilated room have been conducted in the past decades. These studies mainly focused on (1) inspecting the influence of different turbulence models, and various numerical schemes and algorithms on the simulation results; and (2) the verification of simulation and experimental results. However, most of these studies concentrated on predicting steady-state indoor air distribution within a ventilated room. In fact, transient behavior of indoor flow characteristics could have great influence on thermal comfort of human beings. For instance, Saeidi and Khodadadi [17] presented a numerical study on an oscillating velocity at the inlet port which leads to transient laminar flow and heat transfer with periodic state within a square cavity with inlet and outlet ports.

The purpose of a ventilating system is to remove heat generation within a room, creating a thermally comfortable environment. One of the active approaches for regulating heat transfer in a convection-dominated cavity system is to use a periodic moving object. For example, Shi and Khodadadi [21] employed CFD method to investigate the effect of an oscillating thin fin on the periodic state of fluid flow and heat transfer in a lid-driven cavity. To remove heat generation within a ventilated room efficiently, the objective of this study is to use dynamic CFD method to investigate the effect of an air-supply guide vane swinging periodically on the indoor air distribution.

## II. Problem Definition and Numerical Methodology

To remove indoor heat generation using the active approach, an air-supply guide vane which can simulate periodic swing with a sin wave is placed near the air-supply inlet of a ventilated room with one inlet and one outlet ports, as shown in Fig. 1(a). Detailed size of the ventilated room and its inlet and outlet ports

C.-C. Tsao is with National Taipei University of Technology, Taipei 10608, Taiwan, R.O.C. (phone: +886-2-8665-8182 ext. 342; fax: +886-2-8665-8180; e-mail: p10093@ temes.com.tw). He is a Ph.D. student in the department of Energy and Refrigerating Air-Conditioning Engineering.

S.-W. Nien is with National Taipei University of Technology, Taipei 10608, Taiwan, R.O.C. (phone: +886911-081-326; fax: +886-2-877-33713; e-mail: nienshihwei@gmail.com). She is a graduate student in the department of Energy and Refrigerating Air-Conditioning Engineering.

W.- H. Chen was with National Taipei University of Technology, Taipei 10608, Taiwan, R.O.C.

Corresponding author: Y.-C. Shih is with National Taipei University of Technology, Taipei 10608, Taiwan, R.O.C. (phone: +886-2-277-12171 ext. 3517; fax: +886-2-273-14919; e-mail: f10958@ ntut.edu.tw). He is a Professor in the department of Energy and Refrigerating Air-Conditioning Engineering.

is displayed in the figure. The outline of the ventilated room employed in this study is modified according to the model room used by the study of Neilson [3]. Moreover, an enlarged view of inlet port and swinging vane is displayed in Fig. 1b, accompanying with the size of each component. The inclined angle of the guide vane with the horizontal is 45° in the initial state. To simulate the heating load within the room, a constant heat flux, $q''$, is imposed on the floor.

The CFD software FLUENT [22], based upon the numerical model of "Finite Volume Method", was employed to simulate the indoor airflow distribution in this study. The governing equations, including the continuity, momentum, energy, and turbulence equations obey the principle of conservation, which can be expressed as the following general form

$$\frac{\partial}{\partial t}(\rho\varphi)+\nabla\bullet\left(\rho\vec{V}\varphi-\Gamma_{\phi,eff}\nabla\varphi\right)=S_{\varphi} \quad (1)$$

where ρ is the air density, $\varphi$ is the dependent variable, $\vec{V}$ is the velocity vector, $\Gamma_{\varphi,eff}$ is the effective diffusion coefficient, and $S_{\varphi}$ is the source term. To simulate the characteristics of turbulent flow, the standard *k-ε* turbulence model was used in this work.

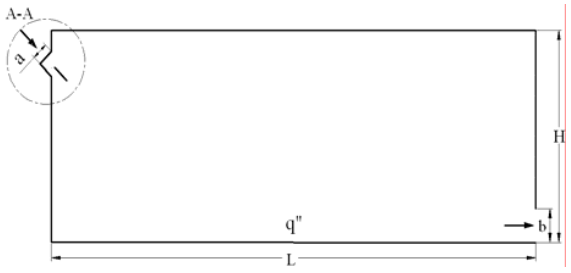


(a)

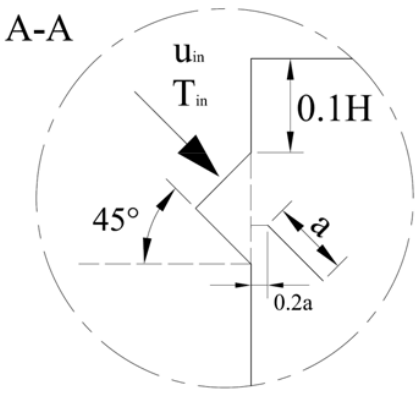


(b)

Fig. 1 Schematic diagram of a model room

The diffusion-convection term of Equation (1) was discretized by the QUICK scheme and the implicit method was utilized to discretize the transient term. After Equation (1) was discretized, the general discretized equation can be written as

$$a_c\varphi_c=\sum a_{nb}\varphi_{nb}+b \quad (2)$$

where $a_c$ and $a_{nb}$ are the discretized coefficients, and *b* is the discretized source term. In Equation (2), subscript *c* represents the grid point under consideration and *nb* is the neighbors of grid point *c*. By employing the iterative scheme of a point implicit (Gauss-Seidel) linear equation solver in conjunction with an algebraic multigrid (AMG) method, thus the pressure, velocity, and turbulence fields can be solved from Equation (2). During the iterative procedure, the PISO algorithm was adopted to solve the pressure-velocity coupling equations.

Regarding the boundary conditions, no-slip condition is used at the wall, and the standard wall functions for the *k-ε* turbulence model are adopted to link the solution variables at the near-wall cells and the corresponding quantities near the wall. Moreover, the turbulence kinetic energy *k* and the turbulence kinetic energy dissipation rate *ε* employed in air supply and air outlet are calculated by the following equations:

$$k=\frac{3}{2}\left(u_{avg}I\right)^2 \quad (3)$$

$$\varepsilon=C_{\mu}^{\frac{3}{4}}\frac{k^{\frac{3}{2}}}{l} \quad (4)$$

$$l=0.07D_h \quad (5)$$

where $u_{avg}$ is the mean flow velocity, $I$ is the turbulence intensity, $D_h$ is the hydraulic diameter and $C_{\mu}$= 0.09.

To simulate room air distribution affected by a swinging guide vane, dynamic meshes were employed in the numerical simulation. Basic conservation equation of the dynamic mesh method is described as follows:

Within an arbitrary control volume *V*, as its boundary moves, the integral form of governing equation is given by

$$\frac{d}{dt}\int_V\rho\phi dV+\int_{\partial V}\rho\phi\left(\vec{u}-\vec{u}_g\right)\cdot d\vec{A}=\int_{\partial V}\Gamma\nabla\phi\cdot d\vec{A}+\int_V S_{\phi}dV \quad (6)$$

where $\partial V$ is the boundary of control volume *V* and $\vec{u}_g$ is the grid velocity of the moving mesh.

## III. Results and Discussion

In this study, the velocity magnitude of 15 m/s and the temperature of 305 K were employed as the boundary conditions at the inlet of air supply. The boundary condition at the exit was set to be pressure outlet with zero gauge pressure. The constant heat flux of 10000 W/m$^2$ was imposed on the floor. Other walls were assumed to be adiabatic. Detailed size of the model room shown in Fig. 1(a) can be referred to [3]. In Fig. 1(b), the inlet width, a, is equal to 0.056 H. The length of the

guide vane was set to be the same as that of inlet width. The grid cell of 23852 was adopted in the numerical simulation.

The guide vane was assumed to swing periodically with a sine wave; as a result, the swing angle, $\theta$, and the angular velocity, $\omega$, of the guide vane are expressed by

$$\theta = \theta_0 + Am \bullet \sin(2\pi ft) \quad (7)$$

$$\omega = Am \bullet 2\pi f \bullet \cos(2\pi ft) \quad (8)$$

where $\theta_0$ is the initial position of the guide vane, $Am$ is the amplitude, $f$ is the frequency and $t$ is the time. To investigate the influence of the amplitude and frequency of the swinging guide vane on the indoor air distribution, three kinds of amplitudes, $Am$ (15°, 30°, and 45°), and three kinds of Stouhal number, $St$ ($5x10^{-4}$, $1x10^{-3}$, and $2x10^{-3}$), to represent the frequency were used in the case study. Stouhal number is given by

$$St = \frac{D_h \cdot f}{u_{in}} \quad (9)$$

where $D_h$ is the hydraulic diameter, $f$ is the frequency and $u_{in}$ is the inlet velocity. There were nine simulating cases in total in this study.

To visualize the transient variation of the velocity and temperature fields with the swing of the guide vane within the model room, the movement of the guide vane is divided into eight periods. The time of the guide vane to swing a cycle is $\tau$. Fig. 2 shows that the positions of the guide vane at eight periods in the case with the amplitude of 45°. The original position of the guide vane has the inclination angle of 45° with the horizontal line. It started to move upward and then moved downward once it hit the dead end. When it hit the other dead end on the downside, it moved upward and returned to the original position to complete one cycle.

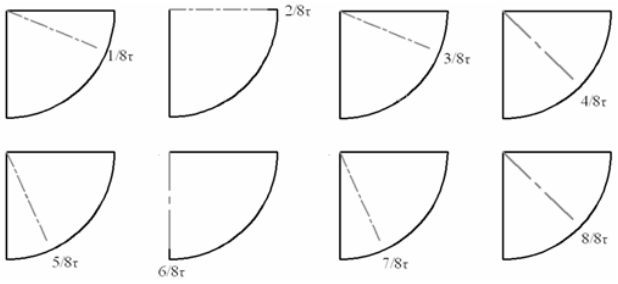


Fig. 2 The position of the guide vane in a cycle ($Am$= 45°)

Fig. 3(a)-(d) show the transient behavior of streamlines and temperature contour for the case of the smallest amplitude and Stouhal number, $St$ (or frequency). Because the cold flow coming from the air-supply inlet injected into the model room, streamlines show two major vortices forming within the model room: a smaller one rotating in clockwise direction developing under the cold jet and a larger one rotating in counter-clockwise direction occupying the model room. The size of the smaller vortex enlarged as the guide vane moving upward, while its size decreased as it moving downward. The larger one had the opposite trend with that of the smaller one. Moreover, the airflow under the cold jet had higher temperature because the smaller vortex was encaged under the cold jet, resulting in the heat accumulation within the smaller vortex. The effect of the swinging guide vane forced the accumulating heat to leave the smaller vortex gradually.

Fig. 4 (a)-(d) show the transient behavior of streamlines and temperature contour for the case of the largest amplitude and Stouhal number, $St$ (or frequency). Initially, two primary vortices developed within the model room similar to previous case. To some extent, the enlargement and decrease of both vortices size in this case were larger than that of previous case due to the effect of large amplitude. Since the time at 6/8 $\tau$, two smaller vortices developed under the cold jet and moved outward gradually. These shedding vortices forced the flow under the cold jet to dispel more quickly. Therefore, these shedding vortices resulting from the large amplitude of the swinging guide vane drove away the accumulating heat under the cold jet more easily and quickly, as shown in the temperature contour of this case.

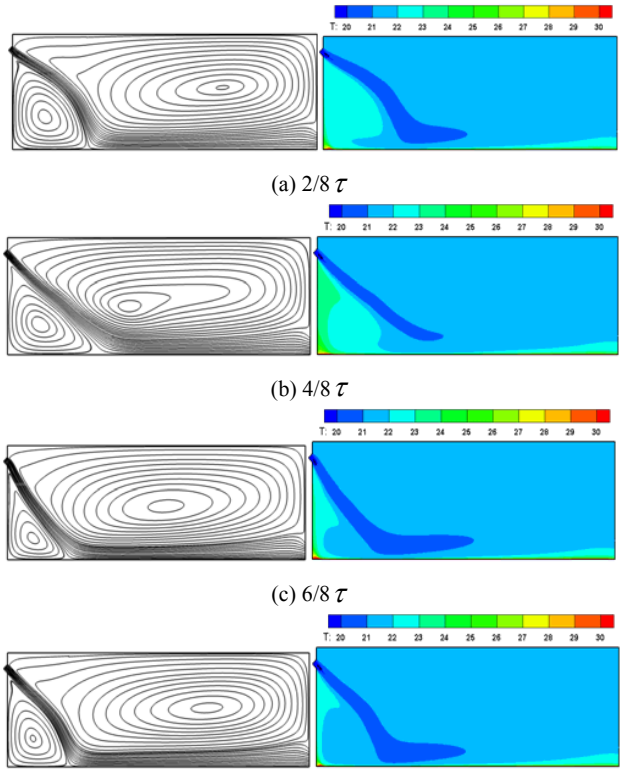

(a) 2/8 $\tau$

(b) 4/8 $\tau$

(c) 6/8 $\tau$

(d) 8/8 $\tau$

Fig. 3 Streamlines (left) and temperature contour (right) ($Am$= 15°, $St$= $5x10^{-4}$)

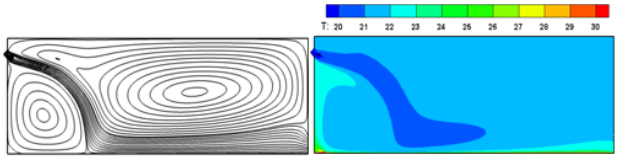

(a) 1/8 $\tau$

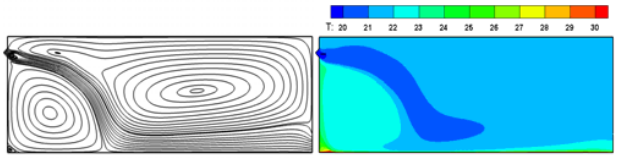

(b) 2/8 $\tau$

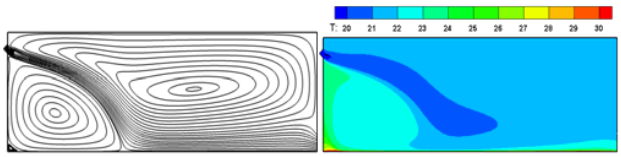

(c) 3/8 $\tau$

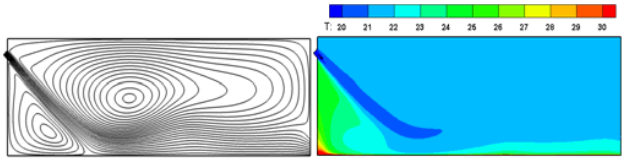

(d) 4/8 $\tau$

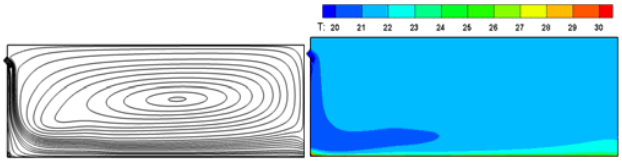

(e) 5/8 $\tau$

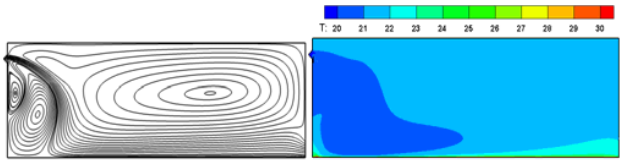

(f) 6/8 $\tau$

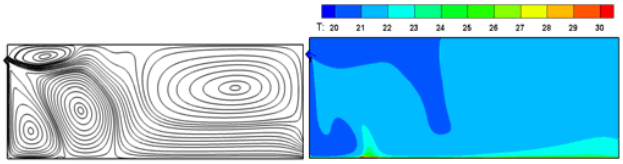

(g) 7/8 $\tau$

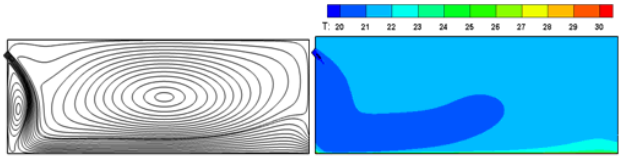

(h) 8/8 $\tau$

Fig. 4 Streamlines (left) and temperature contour (right) ($Am$= 45°, $St$= 2x10$^{-3}$)

Fig. 5(a)-(c) compare the streamlines and temperature contour of three kinds of $St$ at the time of 7/8 $\tau$ when the amplitude is the largest. Among the three cases, it can found that two vortices developing under the cold jet and they started to shed outward as the guide vane moved upward. As a result, the heat flux imposed by floor was removed gradually through the outlet.

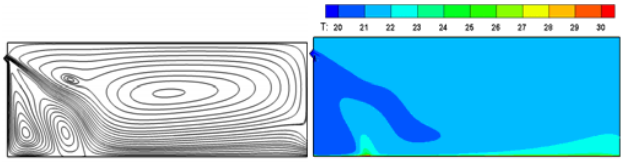

(a) $St$= 5x10$^{-4}$

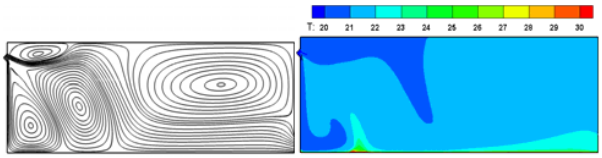

(b) $St$= 1x10$^{-3}$

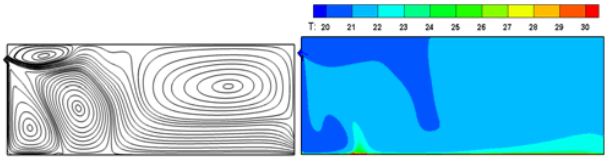

(c) $St$= 2x10$^{-3}$

Fig. 5 Streamlines (left) and temperature contour (right) ($Am$= 45°, 7/8 $\tau$ )

To assess the effect of amplitude and frequency of the swing guide vane on the heat transfer performance within the model room. The instantaneous Nusselt number along the floor is given by

$$Nu_f(\tau) = \frac{h \cdot L}{k} \quad (10a)$$

$$h = \frac{q''}{(\overline{T_f}(\tau) - T_{in})} \quad (10b)$$

where $\overline{T_f}$ is the instantaneous average floor temperature. The average Nusselt number, $\overline{\mathrm{Nu}_f}$, shown in Fig. 7 is the average of the instantaneous Nusselt number in a cycle. Cases 1-3 of Fig. 7 represent $St$=5x10$^{-4}$, 1x10$^{-3}$, and 2x10$^{-3}$, respectively when $Am$ is fixed to be 45°. Cases 4-6 have the condtions of $Am$= 30° and three different values of $St$. Cases 7-9 keep $Am$ to

be 15° with three different *St*. The results disclosed that the average Nusselt number was not affected by *St* when *Am* was fixed. However, $\overline{Nu}_f$ increased with the increase of *Am* because large *Am* resulted in two vortices developing under the cold jet and these shedding vortices enhanced the heat transfer performance within the model room.

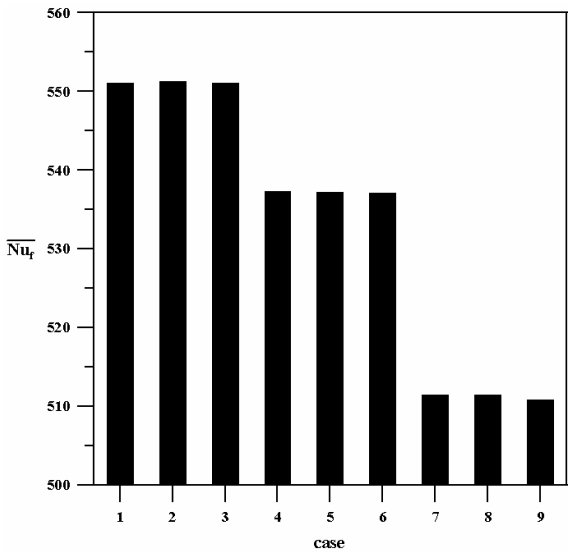


Fig. 6 Comparison of average Nusselt number for each case

## IV. Conclusion

This study conducted a numerical study to investigate the impact of the amplitude and frequency of a swing guide vane on the heat transfer performance in a model room. According to the numerical results, the following conclusions can be drawn:

(1) As the inlet cold flow injects into the model room, one smaller vortex develops under the cold jet and the other larger vortex occupies the model room.
(2) When *Am* is larger, two smaller vortices develop under the cold jet and shed outward continuously. As a result, the heat load imposed by the floor is more easily removed by these shedding vortices.
(3) The average Nusselt number increases with the increase of the amplitude of the swing guide vane. However, it does not affected by the swing frequency.

## Acknowledgment

The support of the National Science Council of Taiwan ROC, through contract number NSC-99-2221 -E-027-033-MY3, is gratefully acknowledged.

## References

[1] ISO 7730, Ergonomics of the Thermal Environment - Analytical Determination and Interpretation of Thermal Comfort Using Calculation of the PMV and PPD Indices and Local Thermal Comfort Criteria, 2005.
[2] ANSI/ASHRAE 55, Thermal Environmental Conditions for Human Occupancy, 2004.
[3] P. V. Nielsen, A. Restivo, and J. H. Whitelaw, "The Velocity Characteristics of Ventilated Rooms," J. Fluids Engineering, vol. 100, pp. 291-298, 1978.
[4] P. V. Nielson, "The Selection of Turbulence Models for Prediction of Room Airflow," ASHRAE Trans., vol. 104, Part. 1B, pp. 1119-1127, 1998.
[5] H. B. Awbi, "Application of Computational Fluid Dynamics in Room Ventilation," Building and Environment, vol. 24, pp. 73-84, 1989.
[6] Awbi, H.B., Ventilation of Buildings, 1st Edition, E & FN SPON, 1991.
[7] Q. Chen, "Computational fluid dynamics for HVAC: success and failures," ASHRAE Transaction, vol. 103(1), pp. 178-187, 1992a.
[8] Q. Chen, "Significant Questions in Predicting Room Air Motion," ASHRAE Transaction, vol. 98, Part. 1, pp. 927-939, 1992b.
[9] Q. Chen, and L. R. Glicksman, "Simplified Methodology to Factor Room Air Movement and the Impact on Thermal Comfort into Design of Radiative, Convective and Hybrid Heating and Cooling Systems," ASHRAE report: RP-927, 1999.
[10] Q. Chen, "Ventilation performance prediction for buildings: A method overview and recent applications," Building and Environment, vol. 44, pp. 848-858, 2009.
[11] S. Murakami, M. Kaizuka, H. Yoshino, and S. Kato, Room air convection and ventilation effectiveness, American Society of Heating, Refrigeration and Air-Conditioning Engineers, Inc. USA., 1992.
[12] S. Murakami, S. Kato, and R. Ooka, "Comparison of Numerical Predictions of Horizontal Nonisothermal Jet in a Room with Three Turbulence Models- k-ε, EVM, ASM, and DSM", ASHRAE Transaction, vol. 100, Part. 2, pp. 697-704, 1994.
[13] Y. Li, and L. Baldacchino, "Implementation of some higher-order convection schemes on non-uniform grids," International Journal for Numerical Methods in Fluids, vol. 21, pp. 1201-1220, 1995.
[14] W. Xu, Q. Chen, and F. T. M. Nieuwstadt, "A New Turbulence Model for Near-Wall Natural Convection", International Journal of Heat and Mass Transfer, vol. 41, pp. 3161-3176, 1998.
[15] Q.-H. Deng, and G.-F. Tang, "Numerical visualization of mass and heat transport for mixed convective heat transfer by streamline and heatline," Int. J. Heat Mass Trans., vol. 45, pp. 2387-2396, 2002.
[16] G. Gan, "Evaluation of Room Air Distribution Systems Using Computational Fluid Dynamics," Energy and Buildings, Vol.23, pp. 83-93, 1995.
[17] S. M. Saeidi, and J. M. Khodadadi, "Forced convection in a square cavity with inlet and outlet ports," Int. J. Heat Mass Transfer, vol. 49, pp. 1896-1906, 2006.
[18] S. L. Sinha, R. C. Arora, and S. Roy, "Numerical Simulation of Two-Dimensional Room Air Flow with and without Buoyancy," Energy and Buildings, vol. 32, pp. 121-129, 2000.
[19] Z. Zhang, W. Zhang, Z. Zhai, and Q. Chen, "Evaluation of various turbulence models in predicting airflow and turbulence in enclosed environments by CFD: Part-2: comparison with experimental data from literature," HVAC&R Research, vol. 13, no. 6, 2007.
[20] A. Stamou, and I. Katsiris, "Verification of a CFD model for indoor airflow and heat transfer," Building and Environment, vol. 41, pp. 1171-1181, 2006.
[21] X. Shi, and J. M. Khodadadi, "Fluid Flow and Heat Transfer in a Lid-Driven Cavity Due to an Oscillating Thin Fin: Transient Behavior," ASME J. Heat Transfer, vol. 126, pp. 924-930, 2004.
[22] ANSYS FLUENT: User's Guide, Release 14.5, ANSYS Inc., USA, 2012.